CORE
Metadata, citation and similar papers at core.ac.uk
Provided by Cronfa at Swansea University

Cronfa - Swansea University Open Access Repository

This is an author produced version of a paper published in:
MATEC Web of Conferences

Cronfa URL for this paper:
http://cronfa.swan.ac.uk/Record/cronfa40730

Paper:
Davey, W., Bache, M., Davies, H. & Thomas, M. (2018). Fatigue Performance of the Novel Titanium Alloy Timetal 407. *MATEC Web of Conferences, 165*, 04001
http://dx.doi.org/10.1051/matecconf/201816504001

This item is brought to you by Swansea University. Any person downloading material is agreeing to abide by the terms of the repository licence. Copies of full text items may be used or reproduced in any format or medium, without prior permission for personal research or study, educational or non-commercial purposes only. The copyright for any work remains with the original author unless otherwise specified. The full-text must not be sold in any format or medium without the formal permission of the copyright holder.

Permission for multiple reproductions should be obtained from the original author.

Authors are personally responsible for adhering to copyright and publisher restrictions when uploading content to the repository.

http://www.swansea.ac.uk/library/researchsupport/ris-support/

Fatigue Performance of the Novel Titanium Alloy Timetal 407

William Davey[1], *Martin* Bache[1,*], *Helen* Davies[1] and *Matthew* Thomas[2]

[1]Institute of Structural Materials, College of Engineering, Bay Campus, Swansea University, Swansea, SA1 8EN, UK
[2]Timet UK, Holdford Road, Birmingham, B6 7BJ, UK

Abstract. Timetal 407 (Ti-407) is a novel titanium alloy formulated as a lower strength, more malleable alloy offering a range of cost reduction opportunities compared with Ti-6-4 (Ti-6Al-4V). An investigation of the room temperature, high cycle and low cycle fatigue properties of Ti-407 is presented. The effect of thermo-mechanical processing on microstructure is characterised and the fatigue properties of a microstructure containing 30-40% primary alpha volume fraction are presented and discussed. The Ti-407 results are compared with data generated from Ti-6-4 processed to provide a similar microstructure, to demonstrate both superior HCF endurance strength and ductility of the former.

1 Introduction

Titanium alloys have been extensively used within the aero-engine sector since the 1950s. The high strength to weight ratio at low to intermediate service temperatures, good corrosion resistance and low density relative to that of other suitable metals, allow the production of lightweight and durable components with applications ranging from the large-scale fan blades and supporting discs at the front of the engine through to relatively small vanes and blades in the high pressure compressor section. The well-established Ti-6-4 (Ti-6Al-4V), the 'workhorse titanium alloy', is still used for a large number of components within the engine, in part due to the range of microstructural forms produced via thermo-mechanical processing that can be tailored to specific applications. Ti-6-4 accounts for 50% of the total titanium production[1]. This alloy delivers an auspicious balance of mechanical properties including good fatigue performance with intermediate fracture toughness and moderately high tensile strength[2]. Over the years much work has been performed to optimise the manufacturing and production of Ti-6-4 components. However, economic competition is forcing more cost-effective production leading to the development of bespoke alloys, better suited for specific components in terms of both mechanical performance and ease of manufacture.

In general, the machinability of titanium and its alloys can be considered to be difficult. Early practitioners in the 1950s believed that "machining of titanium and its alloys would always be a problem, no matter what techniques are employed to transform this metal into chips[3]". More recent workers in the 1980s, when referring to the same issues, stated that "this is still true in so far as cutting tool materials are concerned[4]." The low thermal conductivity of titanium increases the temperature at the tool/workpiece interface, decreasing the tool life. When machining Ti-6-4, about 80% of the heat generated is conducted into the tool and is concentrated on the cutting edge and tool face. Additionally, titanium is highly chemically reactive. This results in the material welding to the cutting tool during machining leading to significantly shorter tool lives. The high strength of titanium which is maintained at elevated temperatures and the relatively low elastic modulus decreases further the machinability. For these reasons, the improvements in machining of titanium alloys has fallen behind the progress seen by other materials in this area[5]. Other alloys such as steels and nickel-based superalloys have benefited from the advancement in the development of cutting tools. This progress includes the use of coated carbides, ceramics, cubic boron nitride and polycrystalline diamond[6]. These cannot be used with titanium, however, because of a strict set of quality criteria driven by the aerospace and automotive industries. The tools need a high coefficient of thermal conductivity, good thermal resistance, high hardness, wear durability and hot hardness. Hence, tungsten carbide tools are used for the vast majority of titanium tooling processes.

TIMET is constantly addressing the need for new bespoke titanium alloys. The focus of the present study was placed on one such alloy, Ti-407. Relative to Ti-6-4, one of the main benefits and most important design features offered by Ti-407 is a significant improvement in ductility, in turn offering superior manufacturability and increased machining speeds with lower contact forces. During machining trials, Ti-407 displayed more than twice the tool life of the baseline Ti-6-4 alloy[7]. Compared to Ti-6-4 the low flow stress, greater malleability and wide process window of Ti-407 should allow it to be processed with fewer reheats, while exhibiting less surface cracking and giving a consistently good surface finish. Optimised Ti-407 manufacturing processes should favour nearer net shape giving higher yields and requiring less machining to finished component. Ti-407 has a slightly higher beta content, making it denser than Ti-6-4. However, by employing suitable designs, components can still be manufactured from Ti-407 as a weight neutral alloy.

Of particular interest, Ti-407 can replace Ti-6-4 in applications where the key design criteria are energy absorption during fracture and HCF endurance limit. The

* Corresponding author: m.r.bache@swansea.ac.uk

© The Authors, published by EDP Sciences. This is an open access article distributed under the terms of the Creative Commons Attribution License 4.0 (http://creativecommons.org/licenses/by/4.0/).

most relevant applications within the gas turbine are, therefore, the engine fan and compressor casings. Due to its relatively low strength, Ti-407 may not be able to replace all Ti-6-4 components, but promisingly, Ti-407 demonstration casings have shown 2.5 times the lateral expansion and absorbed more than twice the impact energy when compared to Ti-6-4[7].

2 Experimental Methods

2.1 Ti-407 production and sampling

The present study utilised Ti-407 alloy (Ti-0.85Al-3.9V-0.15O-0.25Si-0.25Fe) in the form of "pancake" forgings processed by TIMET. Billet sections were cut into six, 60° degree segments. These were then forged into the pancake form which is displayed in Figure 1, from which the mechanical test specimen blanks were extracted from the central regions.

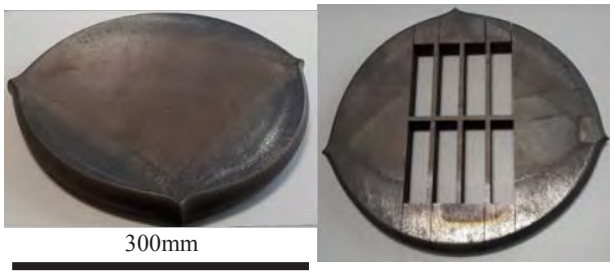

Fig. 1. A pancake forging and specimen blank extraction.

Heat treatment trials were conducted in order to establish a solution treatment temperature that would generate a bimodal microstructure with approximately 30-40% primary alpha (α_p) volume fraction. This goal was based on results from previous research[8] which suggested that this specific volume fraction provided the optimum fatigue performance. Increasing content has been shown to increase tensile plasticity[9], refine the microstructure and limit the formation of areas of common orientation [10]. Whilst α_p within a lamellar matrix does offer these advantages, the percentage volume must be carefully restricted since beyond a critical volume, ductility ceases to improve and alloy element partitioning takes place. This degrades the basic strength of the lamellar constituent of the microstructure, therefore resulting in a decrease in fatigue life.

A SNOL 1.8Kw electric furnace was employed for microstructure trials, with two calibrated N type thermocouples in contact with the specimens (15x15mm cubes). The temperatures were constantly monitored throughout the duration of the heat treatments using calibrated Fluke thermometers. Samples were subjected to three different solution heat treatments, each for a two- hour period;

- 820°C producing 50% α_p volume fraction
- 840°C producing 30% α_p volume fraction
- 860°C producing 20% α_p volume fraction.

The resultant microstructures are displayed in Figure 2 along with image analysis based measurements of the α_p volume fractions.

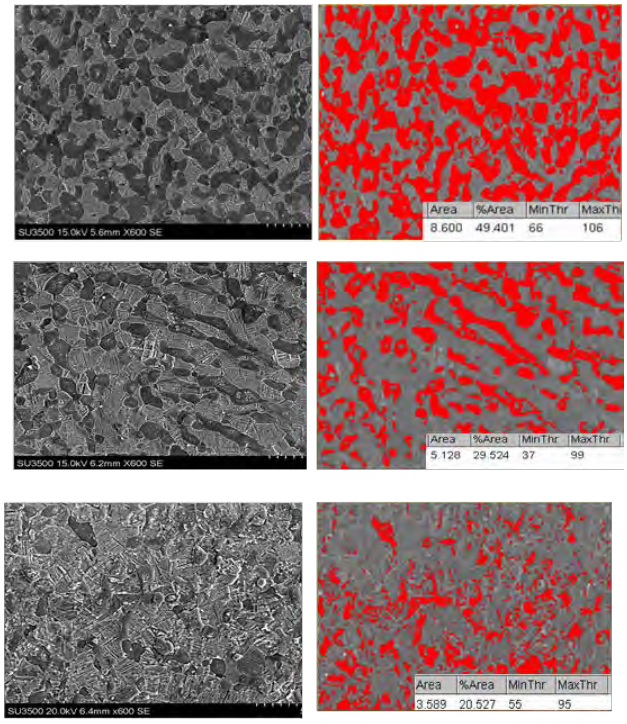

Fig. 2. Microstructures generated under the three solution heat treatments.

All mechanical specimen blanks were subsequently heat treated at 840°C for two hours, followed by an eight-hour aging treatment at 500°C. The 30% volume fraction of α_p grains demonstrated an average α_p grain diameter of 10 to 15 microns. The blanks were then machined using CNC turning operations into plain cylindrical specimens suitable for tensile and fatigue experiments, Figure 3 and Figure 4. A non-contacting shadowgraph was employed to measure the co-axiality of the test pieces and the critical dimensions of the parallel gauge section according to the guidance of aerospace based fatigue test standards [11].

Fig. 3. Examples of post heat treated blank, CNC machined cylinder and final test piece.

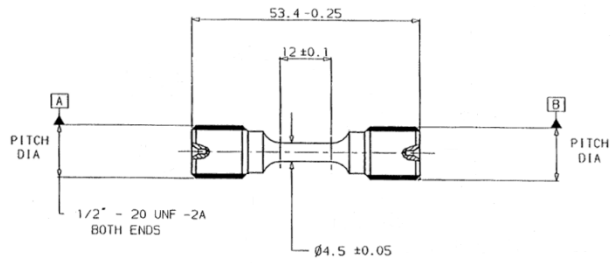

Fig. 4. Mechanical specimen geometry.

2.2 Ti-6-4 production and sampling

In order to provide a comparison between HCF performance, Ti-6-4 blanks were extracted from similar forged pancake material stock. The same method was employed to determine a heat treatment temperature that would produce a α_p volume fraction of approximately 30%. Two temperatures were trialled, again with the samples subject to a 2 hour solution treatment:

- 950°C producing ~30% α_p volume fraction.
- 960°C producing ~40% α_p ha volume fraction

The resultant microstructures are displayed in Figure 5 along with image analysis based on measurements of the α_p volume fraction.

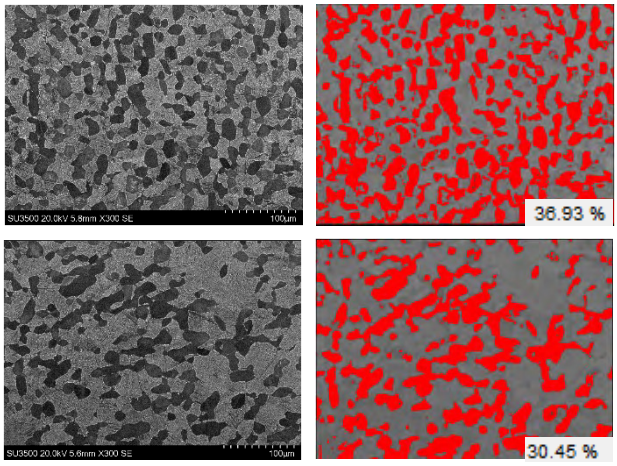

Fig. 5. Ti-6-4 microstructures generated from the two different heat treatments.

It is emphasised that the 950°C heat treatment we ultimately employed provides a bespoke microstructure, i.e. non-standard for typical aero-engine casing applications. Instead, this offered an academic comparison with Ti-407 processed to the same 30% α_p content.

2.3 HCF and LCF Testing

High cycle fatigue (HCF) tests were conducted on an Amsler vibrophore resonance machine at a load ratio of R=0 under room temperature, using a sinusoidal waveform with a frequency of 100Hz. Low cycle fatigue (LCF) tests, again under R=0 at room temperature, employing a 15 cycle per minute trapezoidal waveform comprising one second linear rise and fall ramps with a one second hold at both peak and minimum load, were performed on various servo-hydraulic test rigs. All test machine load cells were calibrated to BS EN ISO 7500-1:2015[12]. In all fatigue tests, complete rupture of the specimen was induced (i.e. no "run-outs" were generated).

3 Results

3.1 Tensile Testing

Key mechanical properties of the Ti-407 pancake material were measured through tensile testing. Following the guidelines of BS EN ISO 2002-1:2005 [13], a strain rate of 0.002/min was applied to define yield, increasing to a rate of 0.01/min to induce fracture. The tensile results are summarised in Table 1.

Table 1. Tensile data for Ti-407.

Attribute	Ti-407
Young's modulus (GPa)	114
Tensile strength (MPa)	764
Yield strength (MPa)	648
Ductility (%)	18

3.2 Fatigue Data and Fractography

The combined fatigue data for Ti-407 generated under LCF and HCF conditions are plotted in Figure 6. Least squares best fit trend lines are superimposed to the individual sets of fatigue data. The range of maximum cyclic stresses assessed under both regimes was identical (with individual tests performed between 500 and 650MPa). This helped to emphasise a significantly stronger response under HCF conditions relative to LCF performance. Figure 7 compares HCF performance between Ti-407 and the non-standard Ti-6-4.

The individual LCF and HCF Ti-407 fatigue fracture surfaces displayed a mixture of surface and subsurface initiation sites, see Figure 8. The sub-surface initiated failures were easily identified by the circular shaped, bright halo formed during sub-surface crack propagation, effectively within a vacuum environment. The fracture surface surrounding the halo, formed after the crack broke through at the surface and now open to oxidation, took a dull appearance. Quasi-cleavage facets were invariably revealed at the centre of the halo marking the precise site of fatigue crack initiation. These relatively flat, facetted regions were orientated near perpendicular to the applied tensile stress axis and were lustrous to the naked eye. Under higher magnification scanning electron microscope (SEM) inspection, the facets were formed of a cluster of elongated features representing the earliest stages of fracture through neighbouring α_p grains, with regions of a more ductile appearance between representing failure of the juxtaposed transformed α/β microstructure, see Figure 9.

3.3 Sub-fracture micro-texture analysis

After noting the predominance of quasi-cleavage facets at the epi-centre of sub-surface crack initiation sites, metallographic sections were prepared immediately below the fracture surface of selected specimens. The polished plane was prepared approximately 5mm sub-fracture, using standard grinding and etch techniques. Electron back scatter diffraction (EBSD) measurements

were taken to generate crystallographic orientation maps extending across the entire specimen gauge section, exemplified by Figure 10. This represents a montage of 70 individual small area scans of approximately 500 x 500 microns conducted with a step size between 2-3 microns. Figure 3.7 shows the inverse pole figures (IPF) relating to this section. A moderate basal plane texture was evident with a preferred basal pole orientation of x3.6 random. The -12-10 and 01-10 maps also indicate a preferential axis of rotation of individual α_p grains.

4. Discussion

From the perspective of ranking fatigue performance, Ti-407 demonstrated a significantly stronger fatigue strength compared to the non-standard form of Ti-6-4 under HCF loading, Figure 7. Therefore, together with superior ductility, machinability and manufacturing properties Ti-407 could be viewed as a promising alternative alloy for aero-engine containment structures. A single solution heat treatment was adopted for the Ti-407 specimens tested during the present study, providing a α_p volume fraction of 30%. The heat treatment trials demonstrated that α_p content can vary across a relatively limited process window. Therefore it would be prudent to extend our fatigue assessment to different variants of the alloy to consider the sensitivity of this mechanical performance to microstructure.

The relatively high HCF strength of Ti-407 is a promising outcome for what is recognised as a comparatively low static strength alloy. Since fatigue mechanisms in general are intimately controlled by the onset of cyclic plasticity, a future investigation into the cyclic yield performance through strain controlled fatigue testing is envisaged. Specifically, with HCF performance in mind, any sensitivity to machining operations and surface finish should also be considered, although it is recognised that the sub-surface failures generated amongst the current data set suggest that these factors may not be controlling crack initiation.

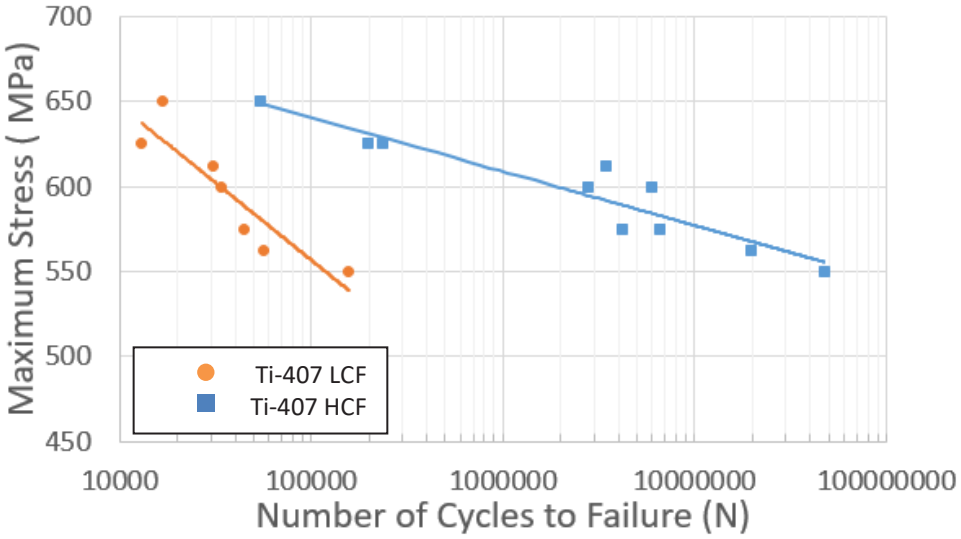

Fig. 6. LCF and HCF data for Ti-407.

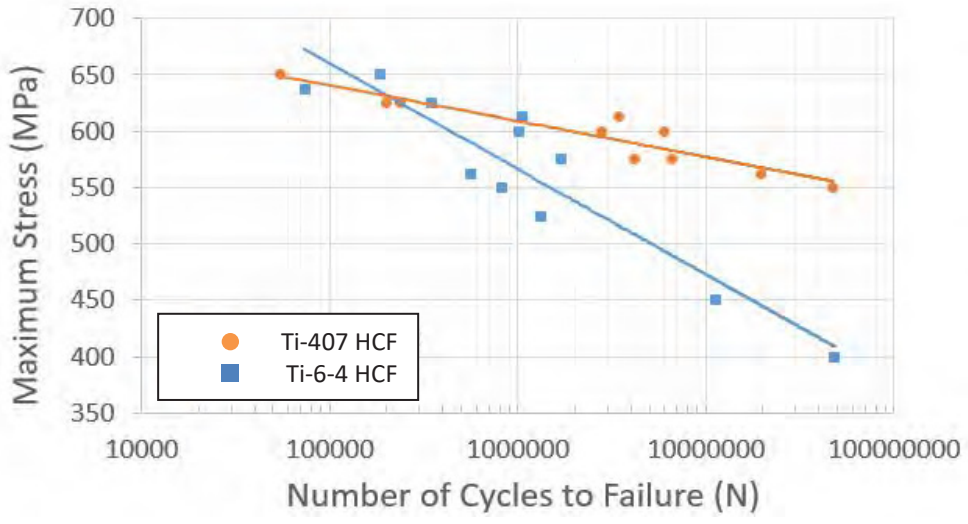

Fig. 7. HCF comparison of Ti-6-4 and Ti-407.

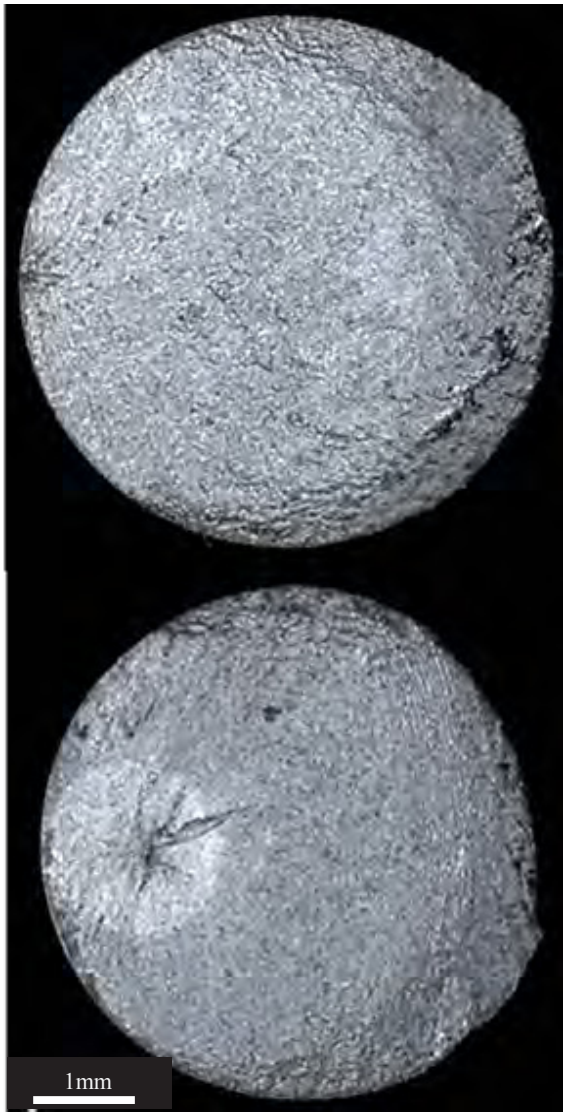

Fig. 8. Examples of surface (top) and sub-surface (bottom) crack initiation sites in Ti-407.

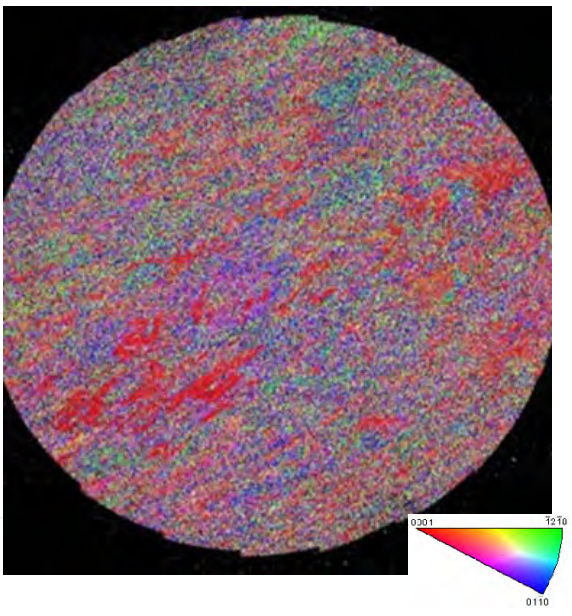

Fig. 10. EBSD orientation map of a sub-fracture section.

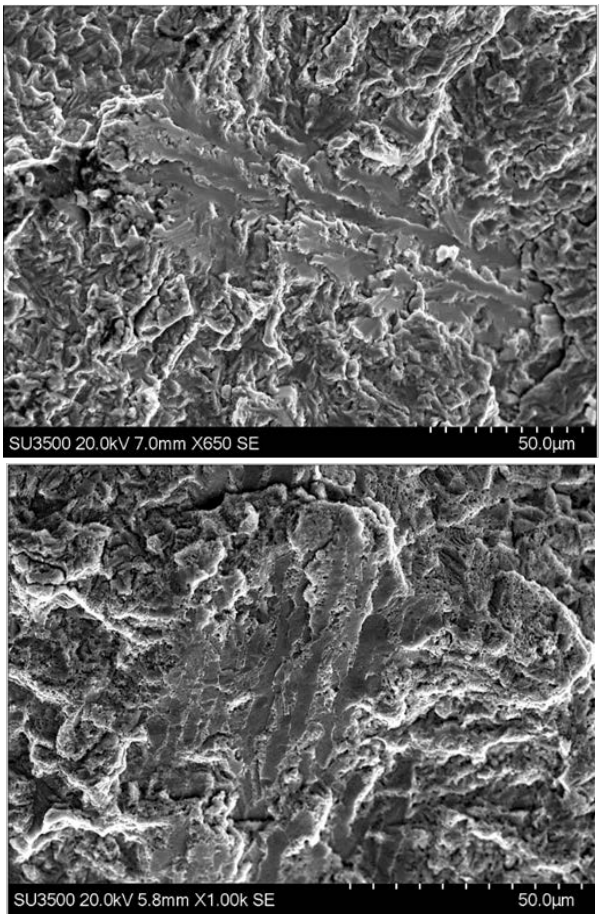

Fig. 9. Sub-surface facet clusters revealing elongated ap α grains exposed on the fracture surface.

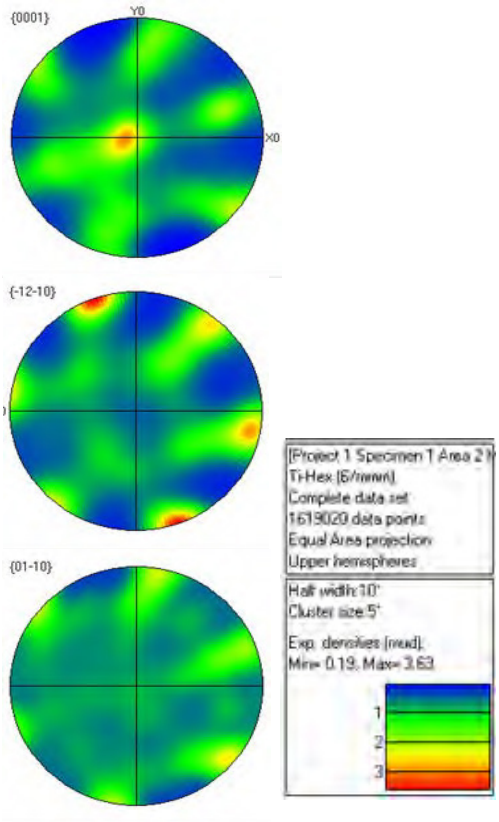

Fig. 11. Pole figures associated with Figure 10.

* Corresponding author: m.r.bache@swansea.ac.uk

Viewing the fatigue behaviour of Ti-407 in isolation (Figure 6), it was interesting to note the greater strength measured under HCF conditions and to consider this in the context of the time-dependent sensitivity of the α/β titanium class of alloys in general. Bache has previously demonstrated that fatigue tests performed on the compressor disc alloy Ti-834 at HCF frequencies induced a stronger response when compared to an LCF based 15cpm waveform[14]. That study went on to assess Ti-834 under a commonly employed two minute dwell waveform and showed forged variants of the alloy were susceptible to "cold dwell". In light of the current investigation on Ti-407, the one second dwell at peak load during the 15cpm LCF experiments appears to induce attributes of a similar dwell response. Although dwell sensitive behaviour would not be considered as a design criterion for containment casings, these results on Ti-407 present an academic interest that will be pursued further in the future.

The appearance and form of the quasi-cleavage faceting in the Ti-407 LCF and HCF fatigue specimens also draws comparisons to Ti-834[15]. At the heart of the initiation sites, facets were discernible associated with individual, elongated α_p grains, which together with multiple neighbouring facets created a cluster. The EBSD characterisation of the microstructural section extracted immediately below the fracture surface of a selected specimen (Figure 3.5), indicated regions shaded in red where α_p grains are all preferentially orientated with their basal plane orthogonal to the applied tensile stress axis. EBSD measurements were also achieved directly from some of the individual facets exposed on the fracture surface. Despite the relatively small α_p grain diameters at less than 15 μm, the regions of common crystallographic orientation provide a much larger "macrozone" or effective structural unit to control deformation and crack initiation mechanisms. Invoking the Stroh model [16] and the subsequent Evans-Bache model[14,17] which applied this theory to the understanding of fatigue failure in a wide selection of α/β titanium alloys, the macrozone with basal orientations perpendicular to the tensile axis would act as a "hard region". The adjacent regions containing a collection of grains with more random orientation would be more favourable for slip deformation thus acting as the neighbouring "soft regions". A process of stress redistribution induces the initial stages of crack initiation within the hard region, eventually observed on the fracture surface as the lustrous cluster of facets lying perpendicular to the tensile stress axis.

The empirically derived Evans-Bache model was later supported by crystal plasticity modelling reported by Zheng et al [18]. Their results suggested that compared to standard cyclic loading, facet formation and crack initiation was encouraged under dwell conditions due to a large increase in the dislocation density within the grains favourably orientated for time-dependent slip. The dwell at peak stress also enables dislocations to escape obstacles over time, resulting in higher intensity dislocation pile-ups at the boundaries between hard and soft grains. In turn this generates higher localised stresses in the hard grains which, in combination with the bulk applied tensile stresses, help the facets to initiate on the basal planes.

The principles behind the Evans-Bache model, but applied to regions or macrozones of common orientation, are represented in the schematic of Figure 12.

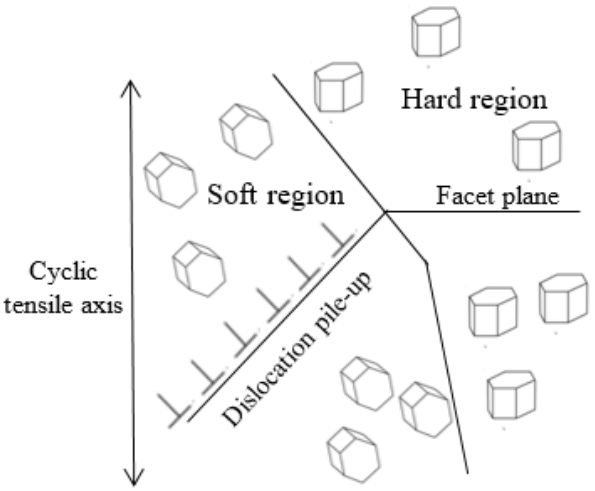

Fig. 12. Adaptation of the Evans-Bache model to incorporate hard and soft regions made up of multiple grains with common basal and random orientations respectively.

It should be emphasised that the material employed for the present study still remains to be optimised for different thermo-mechanical processing routes. Therefore, the microstructural condition produced via the relatively simple billet to pancake forging would not prevail in engineering components. This is particularly true for thin walled containment structures that would probably utilise ring-rolling techniques. The general micro-texture and presence or otherwise of macrozones could be different in the component material variants and so further fatigue assessments will be required.

5. Conclusions

The following conclusions were drawn from the present programme of research:

- The novel alloy Ti-407 could offer a cost-effective replacement for Ti-6-4 engine fan and compressor casings due to its ease of manufacture.
- Ti-407 offers superior HCF fatigue strength despite a relatively low UTS.
- HCF strength is greater than that measured under LCF loading, suggesting Ti-407 fatigue behaviour may be subject to dwell sensitivity.
- Quasi-cleavage facets were invariably noted at crack initiation sites, including examples of sub-surface failures.
- Clusters of facets revealed the underlying microstructure, including elongated α_p grains with transformed product between.
- EBSD defined regions of grains with common basal plane orientation.

6. Acknowledgements

The current research was funded under the EPSRC Rolls-Royce Strategic Partnership in Structural Metallic Systems for Gas Turbines (grants EP/H500383/1 and EP/H022309/1). The provision of materials and supporting information from TIMET UK is gratefully acknowledged. Mechanical tests were performed at Swansea Materials Research and Testing Ltd. (SMaRT).

7. References

1. R. Wood and R. Favor, *Titanium Alloys Handbook*, MCIC-HB-002, Battelle (1972)
2. www.timet.com. [Accessed: 31-Oct-2017].
3. H. Siekmann, Tool Eng., **34**, no. 1, pp. 78–82, (1995)
4. R. Komanduri and W. Reed, Wear, **92**, no. 1, pp. 113–123, (1983)
5. E.O. Ezugwu and Z.M. Wang, *J.* Mater. Process. Technol., **68**, no. 3, pp. 262–274, (1997)
6. M. Rahman, Y.S. Wong and A.R. Zareena, JSME International Journal Series C, **46**, no. 1. pp. 107–115, (2003)
7. S. James, Y. Kosaka, R. Thomas and P. Garratt, *13th International conference on titanium,* Eds. Venkatesh et al, pp.721-725, TMS, (2016)
8. G.Q. Wu, C.L. Shi, W. Sha, A.X. Sha and H.R. Jiang, Mater. Des., **46**, pp. 668–674, (2013)
9. G. Lütjering, Mater. Sci. Eng. A, **243**, no. 1–2, pp. 32–45, (1998)
10. M.T. Whittaker, W.J. Evans, R. Lancaster, W. Harrison and P.S. Webster, Int. J. Fatigue, **31**, no. 11–12, pp. 2022–2030, (2009)
11. J. Krautkräm et al, J. Appl. Phys., **58**, no. 3, pp. 6737–6741, (2006)
12. BS EN ISO 7500-1: *Metallic materials. Verification of static uniaxial testing machines. Tension/compression testing machines. Verification and calibration of the force-measuring system* (2004).
13. BS EN 2002:1, *Metallic Materials - Test Methods: Tensile testing at ambient temperature* (2005)
14. M.R. Bache, Int. J. Fatigue, **25**, pp. 1079–1087, 2003.
15. L. Germain and M.R. Bache, Ti 2007 Science and Technology, **2,** Eds Ninomi et al, Japan Institute of Metals 2007 pp. 953-956 (2015)
16. A. Stroh, *Proc. R. Scociety London A Mathmatical,* Phys. Eng. Sci., **223**, no. 1154, pp. 404–414, (1954)
17. W.J. Evans and M.R. Bache, Titanium '92 Science and Technology, **3**, Eds Froes and Caplan pp.1693-1700, TMS, (1993)
18. Z. Zheng, D.S. Balint and F.P.E. Dunne, Int. J. Plast., **87**, pp. 15–31, (2016)

* Corresponding author: m.r.bache@swansea.ac.uk